

Throughput Maximization for UAV-Enabled Wireless Powered Communication Networks

(Invited Paper)

Lifeng Xie*, Jie Xu*, and Rui Zhang†

*School of Information Engineering, Guangdong University of Technology

†Department of Electrical and Computer Engineering, National University of Singapore

E-mail: lifengxie22039@gmail.com, jiexu@gdut.edu.cn, elezhang@nus.edu.sg

Abstract—This paper studies an unmanned aerial vehicle (UAV)-enabled wireless powered communication network (WPCN), in which a UAV is dispatched as a mobile access point (AP) to serve a set of ground users. The UAV employs the radio frequency (RF) signals based wireless power transfer (WPT) to charge the users in the downlink, and the users use the harvested RF energy to send individual information back to the UAV in the uplink. Unlike the conventional WPCN with fixed APs, the UAV-enabled WPCN can exploit the mobility of the UAV via trajectory optimization, jointly with the wireless resource allocation, to improve the system performance. In particular, we aim to maximize the uplink common throughput among all ground users over a particular finite time period, subject to the UAV’s maximum speed constraint and the users’ energy harvesting constraints. The decision variables include the UAV’s trajectory design, as well as the UAV’s downlink power allocation for WPT and the users’ uplink power allocation for wireless information transfer (WIT). This problem is non-convex and thus very difficult to be solved optimally. To overcome this issue, we first consider a special case when the maximum UAV speed constraint is ignored, and obtain the optimal solution to this relaxed problem. The optimal solution shows that the UAV should hover above a finite number of ground locations over time for downlink WPT, and then hover above each user at different time for uplink WIT. Next, based on the optimal multi-location-hoovering solution to the relaxed problem, we propose the successive hover-and-fly trajectory, jointly with the downlink and uplink power allocation, to efficiently solve the original problem with the maximum UAV speed constraint. Numerical results show that the proposed UAV-enabled WPCN achieves much higher uplink common throughput than the conventional WPCN with fixed-location AP.

I. INTRODUCTION

Radio frequency (RF) signals based wireless power transfer (WPT) has emerged as a promising solution to provide convenient and sustainable energy supply to low-power wireless devices (WDs) in future Internet-of-things (IoT) networks [1]. The emergence of WPT motivates a new type of self-sustainable wireless networks, namely the wireless powered communication network (WPCN), in which dedicated access points (APs) are deployed (at fixed locations conventionally) to charge a set of WDs via WPT in the downlink, and the WDs can use the harvested energy to send information back to the AP in the uplink [1].

The implementation of the conventional WPCN with fixed APs, however, faces several technical challenges. First, due to the severe propagation loss of RF signals over distance,

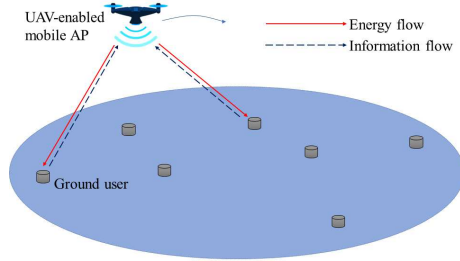


Fig. 1. Illustration of the UAV-enabled WPCN.

the end-to-end WPT efficiency is generally low when the distance from AP to intended WDs becomes large. Next, the conventional WPCN faces the so-called “doubly near-far” problem, i.e., far-apart WDs from the AP receive much lower RF energy in the downlink WPT, but they need to use much higher transmit power in the uplink wireless information transfer (WIT) to achieve the same communication rate as nearby WDs. The doubly near-far problem leads to severe user fairness issue among different WDs that are geographically distributed over a large area. In the literature, various approaches have been proposed to overcome these issues, some examples including adaptive time and power allocation [2], multi-antenna beamforming [3]–[6], and user cooperation [7], [8]. Different from these existing works focusing on link-level approaches, this paper provides an alternative system-level solution, by proposing a new unmanned aerial vehicle (UAV)-enabled WPCN architecture that exploits UAVs in the sky as mobile APs.

UAVs have found abundant industrial and commercial applications in, e.g., cargo delivery, aerial surveillance, filming, plant protection, and wireless industry. Recently, UAV-assisted wireless communications have attracted a lot of research interests [9]. For example, UAVs can be utilized as mobile relays to help information exchange between far-apart ground users [10], and can also be used as mobile base stations (BSs) to help enhance the wireless coverage and/or increase the network capacity for ground mobile subscribers [11]–[14]. Furthermore, UAV-enabled WPT has been proposed in [15], [16], in which UAVs are used as mobile energy transmitters to charge low-power WDs on the ground. By exploiting the fully controllable mobility, UAVs can properly adjust the locations over time (a.k.a. the trajectory) to reduce

the distances with intended ground users, thus improving the efficiency for wireless communication and WPT.

Motivated by the UAV-assisted wireless communications and the UAV-enabled WPT, this paper pursues a unified study of both of them by considering a UAV-enabled WPCN as shown in Fig. 1, in which a UAV is dispatched as a mobile AP to charge a set of ground users in the downlink via WPT, and the users use the harvested RF energy to send individual information back to the UAV in the uplink. We investigate how to optimally exploit the UAV mobility via trajectory optimization, jointly with the wireless resource allocation, in order to maximally improve the performance of WPCN. We aim to maximize the uplink common throughput among all ground users over a particular time period, by jointly optimizing the UAV's trajectory, as well as the UAV's downlink power allocation for WPT and the users' uplink power allocation for WIT. However, due to the coupling between the UAV trajectory and the power allocation, this problem is non-convex and very difficult to be solved optimally.

To tackle this difficulty, we first consider a relaxed problem without the UAV's maximum speed constraint. We show that strong duality holds between this problem and its Lagrange dual problem, and thus it can be solved optimally via the Lagrange dual method. The optimal solution shows that the UAV should hover above a finite number of ground locations over time for downlink WPT, and then hover above each user at different time for uplink WIT, with optimal hovering time allocation and power allocation for each location. Next, we consider the original problem with the maximum UAV speed constraint. Based on the multi-location-hovering solution to the relaxed problem above, we efficiently solve the original problem by proposing a *successive hover-and-fly trajectory* design, jointly with the downlink and uplink power allocation. The proposed solution is shown to be asymptotically optimal for the original problem when the time duration becomes large. Finally, we present numerical results to validate the performance of our proposed UAV-enabled WPCN. It is shown that the joint trajectory and wireless resource allocation design significantly improves the uplink common throughput performance, as compared to the conventional WPCN with the AP fixed at a given location.

II. SYSTEM MODEL AND PROBLEM FORMULATION

As shown in Fig. 1, we consider a UAV-enabled WPCN, in which a UAV is dispatched to charge a set of K ground users via WPT in the downlink, and each user $k \in \mathcal{K} \triangleq \{1, \dots, K\}$ uses its harvested energy to send individual information back to the UAV in the uplink. Suppose that each user $k \in \mathcal{K}$ has a fixed location on the ground, which is denoted by $(x_k, y_k, 0)$ in a three-dimensional (3D) Cartesian coordinate system, where $\mathbf{w}_k = (x_k, y_k)$ is defined for notational convenience. The users' locations are *a-priori* known by the UAV for trajectory design and wireless resource allocation.

We focus on the WPCN over a particular time period $\mathcal{T} \triangleq (0, T]$ with finite duration T , during which the UAV flies horizontally at a fixed altitude $H > 0$ (e.g., several meters). At

any given time instant $t \in \mathcal{T}$, let $\mathbf{q}(t) = (x(t), y(t))$ denote the location of the UAV projected on the horizontal plane. Accordingly, the distance from the UAV to user k is expressed as

$$d_k(\mathbf{q}(t)) = \sqrt{\|\mathbf{q}(t) - \mathbf{w}_k\|^2 + H^2}, \quad (1)$$

where $\|\cdot\|$ denotes the Euclidean norm of a vector. By denoting the maximum UAV speed in practice as $V_{\max} > 0$, then we have

$$\sqrt{\dot{x}^2(t) + \dot{y}^2(t)} \leq V_{\max}, \forall t \in \mathcal{T}, \quad (2)$$

where $\dot{x}(t)$ and $\dot{y}(t)$ denote the time-derivatives of $x(t)$ and $y(t)$, respectively. Note that the UAV can freely choose the initial location $\mathbf{q}(0)$ and the final location $\mathbf{q}(T)$ here.

As the UAV flies at a fixed altitude H of several meters, the wireless channels between the UAV and the K ground users are generally line-of-sight (LoS) dominated. In this case, it is practically reasonable to consider the free-space path loss model, as commonly adopted in the literature [10], [15]. Accordingly, the channel power gain between the UAV and user k at time instant $t \in \mathcal{T}$ is

$$h_k(\mathbf{q}(t)) = \beta_0 d_k^{-2}(\mathbf{q}(t)) = \frac{\beta_0}{\|\mathbf{q}(t) - \mathbf{w}_k\|^2 + H^2}, \forall k \in \mathcal{K}, \quad (3)$$

where β_0 denotes the channel power gain at a reference distance of $d_0 = 1\text{m}$.

We consider a time-division multiple access (TDMA) protocol, in which the downlink WPT and uplink WIT are implemented over the same frequency band but at different time instants. At any time instant $t \in \mathcal{T}$, we use the indicators $\rho_k(t) \in \{0, 1\}, \forall k \in \{0\} \cup \mathcal{K}$, to denote the transmission mode of this system. We use $\rho_0(t) = 1$ and $\rho_k(t) = 0, \forall k \in \mathcal{K}$, to indicate the downlink WPT mode, in which the UAV transmits RF signals to charge the K users simultaneously; furthermore, we use $\rho_k(t) = 1, k \in \mathcal{K}$, and $\rho_j = 0, \forall j \in \{0\} \cup \mathcal{K}, j \neq k$, to represent the uplink WIT mode for user k , in which user k sends its information back to the UAV. It follows that $\sum_{k=0}^K \rho_k(t) = 1, \forall t \in \mathcal{T}$.

First, consider the downlink WPT mode at time instant $t \in \mathcal{T}$, in which $\rho_0(t) = 1$, and $\rho_k(t) = 0, \forall k \in \mathcal{K}$. Let $P(t)$ denote the transmit power of the UAV. Accordingly, the harvested power at each user $k \in \mathcal{K}$ is

$$\begin{aligned} E_k(\rho_0(t), \mathbf{q}(t), P(t)) &= \eta \rho_0(t) P(t) h_k(\mathbf{q}(t)) \\ &= \frac{\eta \beta_0 \rho_0(t) P(t)}{\|\mathbf{q}(t) - \mathbf{w}_k\|^2 + H^2}, \end{aligned} \quad (4)$$

where $0 < \eta \leq 1$ denotes the RF-to-direct current (DC) energy conversion efficiency at the energy harvester of each user. Therefore, the total harvested energy at user k over the whole period of duration T is given as

$$\hat{E}_k(\{\rho_0(t), \mathbf{q}(t), P(t)\}) = \int_0^T E_k(\rho_0(t), \mathbf{q}(t), P(t)) dt. \quad (5)$$

Next, consider the WIT mode for user $k \in \mathcal{K}$ at time instant $t \in \mathcal{T}$ with $\rho_k(t) = 1$, and $\rho_j(t) = 0, \forall j \in \{0\} \cup \mathcal{K}, j \neq k$. Let $Q_k(t)$ denote the transmit power of user k for the uplink WIT to the UAV. Accordingly, the achievable data rate from

user k to the UAV (in bps/Hz) is expressed as

$$\begin{aligned} r_k(\rho_k(t), \mathbf{q}(t), Q_k(t)) &= \rho_k(t) \log_2 \left(1 + \frac{Q_k(t)h_k(\mathbf{q}(t))}{\sigma^2} \right) \\ &= \rho_k(t) \log_2 \left(1 + \frac{Q_k(t)\gamma}{\|\mathbf{q}(t) - \mathbf{w}_k\|^2 + H^2} \right), \end{aligned} \quad (6)$$

where σ^2 denotes the noise power at the information receiver of the UAV, and $\gamma \triangleq \beta_0/\sigma^2$ is the reference signal-to-noise ratio (SNR).

Therefore, the data-rate throughput of user k over the duration T (in bits/Hz) is given as

$$R_k(\{\rho_k(t), \mathbf{q}(t), Q_k(t)\}) = \int_0^T r_k(\rho_k(t), \mathbf{q}(t), Q_k(t)) dt. \quad (7)$$

Note that for the purpose of exposition, we consider the transmit power consumption as the sole energy budget at each user for the uplink WIT. In this case, the total energy consumption at user $k \in \mathcal{K}$ is

$$\hat{Q}_k(\{\rho_k(t), Q_k(t)\}) = \int_0^T \rho_k(t) Q_k(t) dt. \quad (8)$$

In order to achieve the self-sustainable operation of this WPCN, each user k 's energy consumption for uplink WIT (i.e., $\hat{Q}_k(\{\rho_k(t), Q_k(t)\})$ in (8)) cannot exceed that harvested from the downlink WPT (i.e., $\hat{E}_k(\{\rho_0(t), P(t), \mathbf{q}(t)\})$ in (5)). As a result, we have the following energy harvesting constraints for the K ground users.

$$\int_0^T \rho_k(t) Q_k(t) dt \leq \int_0^T E_k(\rho_0(t), \mathbf{q}(t), P(t)) dt, \forall k \in \mathcal{K}. \quad (9)$$

In this work, our objective is to maximize the uplink common throughput among all users (i.e., $\min_{k \in \mathcal{K}} R_k(\{\rho_k(t), \mathbf{q}(t), Q_k(t)\})$) subject to the maximum UAV speed constraint in (2) and the K users' energy harvesting constraints in (9). The decision variables include the UAV trajectory $\{\mathbf{q}(t)\}$, the transmission mode $\{\rho_k(t)\}$, the transmit power $\{P(t)\}$ for downlink WPT, and $\{Q_k(t)\}$ for uplink WIT. In particular, the problem of our interest is mathematically formulated as

$$\begin{aligned} (P1) : \max_{\{\rho_k(t), P(t), Q_k(t), \mathbf{q}(t)\}} & \min_{k \in \mathcal{K}} R_k(\{\rho_k(t), \mathbf{q}(t), Q_k(t)\}) \\ \text{s.t. } & 0 \leq P(t) \leq P_{\text{peak}}, \forall t \in \mathcal{T} \end{aligned} \quad (10)$$

$$Q_k(t) \geq 0, \forall k \in \mathcal{K}, t \in \mathcal{T} \quad (11)$$

$$\rho_k(t) \in \{0, 1\}, \forall k \in \{0\} \cup \mathcal{K}, t \in \mathcal{T} \quad (12)$$

$$\sum_{k=0}^K \rho_k(t) = 1, \forall t \in \mathcal{T} \quad (13)$$

(2) and (9),

where P_{peak} in (10) denotes the peak transmit power at the UAV for downlink WPT.

It is observed that for problem (P1), the objective function and the constraints (9) and (12) are all non-convex, due to the coupling of variables $\rho_k(t)$, $\mathbf{q}(t)$, and $P(t)$ (or $Q_k(t)$), as well as the binary constraints on $\rho_k(t)$'s. Therefore, (P1) is a non-convex optimization problem. Furthermore, (P1) contains an infinite number of optimization variables over continuous time. For these reasons, problem (P1) is very difficult to be

solved optimally. To tackle this difficulty, in section III we first optimally solve the following relaxed problem by ignoring the maximum UAV speed constraint in (2).

$$\begin{aligned} (P2) : \max_{\{\rho_k(t), P(t), Q_k(t), \mathbf{q}(t)\}} & \min_{k \in \mathcal{K}} R_k(\{\rho_k(t), \mathbf{q}(t), Q_k(t)\}) \\ \text{s.t. } & (10), (11), (12), (13), \text{ and (14).} \end{aligned}$$

In section IV, we propose an efficient solution to the original problem (P1) based on the optimal solution obtained for (P2). Note that due to the space limitation, in this paper we have omitted all the proofs, which will be shown later in the journal version.

III. OPTIMAL SOLUTION TO PROBLEM (P2)

By introducing an auxiliary variable R , problem (P2) can be equivalently expressed as

$$\begin{aligned} (P2.1) : \max_{\{\rho_k(t), P(t), Q_k(t), \mathbf{q}(t)\}, R} & R \\ \text{s.t. } & \int_0^T r_k(\rho_k(t), \mathbf{q}(t), Q_k(t)) dt \geq R, \forall k \in \mathcal{K} \quad (14) \\ & (9), (10), (11), (12), \text{ and (13).} \end{aligned}$$

Although problem (P2.1) is still non-convex, one can easily show that it satisfies the so-called time-sharing condition in [17]. Therefore, the strong duality holds between (P2.1) and its Lagrange dual problem. As a result, we can optimally solve (P2.1) by using the Lagrange dual method.

Let $\lambda_k \geq 0$ and $\mu_k \geq 0$, $k \in \mathcal{K}$, denote the dual variables associated with the k -th constraints in (14) and (9), respectively. For notational convenience, we define $\boldsymbol{\lambda} = [\lambda_1, \lambda_2, \dots, \lambda_K]$ and $\boldsymbol{\mu} = [\mu_1, \mu_2, \dots, \mu_K]$. The partial Lagrangian of (P2.1) is

$$\begin{aligned} \mathcal{L}(\{\rho_k(t), P(t), Q_k(t), \mathbf{q}(t)\}, R, \boldsymbol{\lambda}, \boldsymbol{\mu}) &= \left(1 - \sum_{k=1}^K \lambda_k \right) R + \sum_{k=1}^K \lambda_k \int_0^T r_k(\rho_k(t), \mathbf{q}(t), Q_k(t)) dt \\ &+ \sum_{k=1}^K \mu_k \left(\int_0^T E(\rho_0(t), \mathbf{q}(t), P(t)) dt - \int_0^T \rho_k(t) Q_k(t) dt \right). \end{aligned} \quad (15)$$

The dual function of (P2.1) is

$$\begin{aligned} g(\boldsymbol{\lambda}, \boldsymbol{\mu}) &= \max_{\{\mathbf{q}(t), Q_k(t), P(t), \rho_k(t)\}, R} \mathcal{L}(\{\rho_k(t), P(t), Q_k(t), \mathbf{q}(t)\}, R, \boldsymbol{\lambda}, \boldsymbol{\mu}) \\ \text{s.t. } & (10), (11), (12) \text{ and (13).} \end{aligned} \quad (16)$$

Lemma 3.1: In order for the dual function $g(\boldsymbol{\lambda}, \boldsymbol{\mu})$ to be upper bounded from above (i.e., $g(\boldsymbol{\lambda}, \boldsymbol{\mu}) < \infty$), it must hold that $\sum_{k=1}^K \lambda_k = 1$.

As a result, the dual problem is given by

$$\begin{aligned} (D2.1) : \min_{\boldsymbol{\lambda}, \boldsymbol{\mu}} & g(\boldsymbol{\lambda}, \boldsymbol{\mu}) \\ \text{s.t. } & \sum_{k=1}^K \lambda_k = 1 \\ & \lambda_k \geq 0, \mu_k \geq 0, \forall k \in \mathcal{K}. \end{aligned}$$

Let the set of $\boldsymbol{\lambda}$ and $\boldsymbol{\mu}$ characterized by the constraints in (D2.1) as \mathcal{X} . As strong duality holds between (P2.1) and (D2.1), we solve (P2.1) by equivalently solving (D2.1). In the following, we first obtain $g(\boldsymbol{\lambda}, \boldsymbol{\mu})$ by solving problem (16) under given $(\boldsymbol{\lambda}, \boldsymbol{\mu}) \in \mathcal{X}$, and then find the optimal $\boldsymbol{\lambda}$ and $\boldsymbol{\mu}$ to minimize $g(\boldsymbol{\lambda}, \boldsymbol{\mu})$.

1) *Obtaining $g(\lambda, \mu)$ by Solving Problem (16) Under Given $(\lambda, \mu) \in \mathcal{X}$:* First, consider problem (16) under any given $(\lambda, \mu) \in \mathcal{X}$. It is evident that problem (16) can be decomposed into the following subproblems.

$$\max_R \left(1 - \sum_{k=1}^K \lambda_k \right) R. \quad (17)$$

$$\begin{aligned} & \max_{\{Q_k(t)\}, \mathbf{q}(t), P(t), \{\rho_k(t)\}} \sum_{k \in \mathcal{K}} \rho_k(t) \varphi_k(\mathbf{q}(t), Q_k(t), \lambda_k, \mu_k) \\ & + \rho_0(t) \phi(\mathbf{q}(t), P(t), \mu_k) \end{aligned} \quad (18)$$

s.t. $0 \leq P(t) \leq P_{\text{peak}}$, $Q_k(t) \geq 0, \forall k \in \mathcal{K}$

$$\rho_k(t) \in \{0, 1\}, \forall k \in \{0\} \cup \mathcal{K}, \sum_{k=0}^K \rho_k(t) = 1, \quad (19)$$

$\forall t \in \mathcal{T}$, where

$$\varphi_k(\mathbf{q}(t), Q_k(t), \lambda_k, \mu_k) = \lambda_k \log_2 \left(1 + \frac{Q_k(t) h_k(\mathbf{q}(t))}{\sigma^2} \right) - \mu_k Q_k(t)$$

$$\phi(\mathbf{q}(t), P(t), \{\mu_k\}) = \sum_{k \in \mathcal{K}} \mu_k \eta P(t) h_k(\mathbf{q}(t)).$$

Here, problem (18) consists of an infinite number of subproblems, each corresponding to one time instant t .

Note that the optimal value of problem (17) is always zero as $1 - \sum_{k \in \mathcal{K}} \lambda_k = 0$. In this case, the optimal solution R^* to problem (17) can be chosen as any arbitrary real number. Therefore, we only need to focus on the subproblems in (18). As the subproblems in (18) are identical for different time instants t 's, we can drop the index t for notational convenience, and denote the optimal solution as $\{Q_k^*\}, \mathbf{q}^*, P^*$, and $\{\rho_k^*\}$.

Notice that for problem (18), there are a total of $K + 1$ feasible choices for $\{\rho_k\}$ due to the constraints in (19). In the following, we solve problem (18) by first obtaining the maximum objective value (and the corresponding optimal Q_k , \mathbf{q} , and P) under each of the $K + 1$ feasible $\{\rho_k\}$, and then comparing them to obtain the optimal $\{\rho_k\}$.

First, consider that $\rho_0 = 1$ and $\rho_k = 0, \forall k \in \mathcal{K}$. In this case, we have the optimal solution to (18) as $P = P_{\text{peak}}$, $Q_k = 0, \forall k \in \mathcal{K}$, and $\mathbf{q} = \bar{\mathbf{q}}_{\omega}^{(\mu)}$, $\omega \in \{1, \dots, \Omega^{(\mu)}\}$, where¹

$$\{\bar{\mathbf{q}}_{\omega}^{(\mu)}\}_{\omega=1}^{\Omega^{(\mu)}} = \arg \max_{\mathbf{q}} \phi(\mathbf{q}, P_{\text{peak}}, \{\mu_k\}) \quad (20)$$

corresponds to the set of optimal hovering locations for downlink WPT, with $\Omega^{(\mu)} \geq 1$ denoting the number of optimal solutions to problem (20). Accordingly, the optimal value of problem (18) is given as $\phi(\{\bar{\mathbf{q}}_{\omega}^{(\mu)}\}, P_{\text{peak}}, \{\mu_k\})$.

Next, consider that $\rho_k = 1$ for any one $k \in \mathcal{K}$ and $\rho_j = 0, \forall j \in \{0\} \cup \mathcal{K}, j \neq k$. In this case, we have the optimal solution to (18) as $P = 0$, $\mathbf{q} = \mathbf{w}_k$, $Q_k = Q^{(\lambda_k, \mu_k)} \triangleq \left(\frac{\lambda_k}{\mu_k \ln 2} - \frac{H^2}{\gamma} \right)^+$, and $Q_j = 0, \forall j \in \mathcal{K}, j \neq k$, where $(x)^+ \triangleq \max(x, 0)$. Accordingly, the optimal value is $\varphi_k(\mathbf{w}_k, Q^{(\lambda_k, \mu_k)}, \lambda_k, \mu_k)$.

By comparing the $K + 1$ optimal values, i.e., $\phi(\{\bar{\mathbf{q}}_{\omega}^{(\mu)}\}, P_{\text{peak}}, \{\mu_k\})$ and $\varphi_k(\mathbf{w}_k, Q^{(\lambda_k, \mu_k)}, \lambda_k, \mu_k)$, $\forall k \in \mathcal{K}$, we have the following proposition.

¹Here, for the non-convex problem (20), we solve it by using a two-dimensional (2D) exhaustive search over the region $[\underline{x}, \bar{x}] \times [\underline{y}, \bar{y}]$, where $\underline{x} = \min_{k \in \mathcal{K}} x_k$, $\bar{x} = \max_{k \in \mathcal{K}} x_k$, $\underline{y} = \min_{k \in \mathcal{K}} y_k$, $\bar{y} = \max_{k \in \mathcal{K}} y_k$. Note that when the optimal solution to problem (20) is non-unique (or $\Omega^{(\mu)} > 1$), we can arbitrarily choose any one of $\bar{\mathbf{q}}_{\omega}^{(\mu)}$'s for obtaining the dual function $g(\lambda, \mu)$.

Proposition 3.1: The optimal solution to problem (18) is obtained by considering following two cases.

- If $\varphi_k(\mathbf{w}_k, Q^{(\lambda_k, \mu_k)}, \lambda_k, \mu_k), \forall k \in \mathcal{K}$, then the UAV works in the downlink WPT mode, i.e.,

$$\rho_0^* = 1, \rho_k^* = 0, P^* = P_{\text{peak}}, Q_k^* = 0, \forall k \in \mathcal{K},$$

$$\mathbf{q}^* \in \{\bar{\mathbf{q}}_1^{(\mu)}, \dots, \bar{\mathbf{q}}_{\Omega^{(\mu)}}^{(\mu)}\}, \quad (21)$$

where \mathbf{q}^* is non-unique when $\Omega^{(\mu)} > 1$.

- Otherwise, the UAV works in the uplink WIT mode for user k^* , i.e.,

$$\begin{aligned} \rho_0^* = 0, \rho_{k^*}^* = 1, \rho_j^* = 0, \forall j \in \mathcal{K}, j \neq k, \\ P^* = 0, Q_{k^*}^* = Q^{(\lambda_{k^*}, \mu_{k^*})}, Q_j^* = 0, \forall j \in \mathcal{K}, j \neq k, \\ \mathbf{q}^* = \mathbf{w}_{k^*}, \end{aligned} \quad (22)$$

where $k^* = \arg \max \varphi_k(\mathbf{w}_k, Q^{(\lambda_k, \mu_k)}, \lambda_k, \mu_k)$.

Note that if any two of the $K + 1$ optimal values (i.e., $\phi(\{\bar{\mathbf{q}}_{\omega}^{(\mu)}\}, P_{\text{peak}}, \{\mu_k\})$ and $\varphi_k(\mathbf{w}_k, Q^{(\lambda_k, \mu_k)}, \lambda_k, \mu_k), \forall k \in \mathcal{K}$) are equal, then the corresponding solutions in (21) and (22) are both optimal for problem (18).

2) *Finding Optimal λ and μ to Solve (D2.1):* Next, we search over (λ, μ) to minimize $g(\lambda, \mu)$ for solving (D2.1). Since the dual problem (D2.1) is always convex but in general non-differentiable, we can use subgradient based methods, such as the ellipsoid method [18], to obtain the optimal λ and μ , denoted by λ^{opt} and μ^{opt} . Note that for the objective function $g(\lambda, \mu)$ in (D2.1), the subgradient with respect to (λ, μ) is

$$\left[Tr_1(\rho_1^*, \mathbf{q}^*, Q_1^*), \dots, Tr_K(\rho_K^*, \mathbf{q}^*, Q_K^*), \right]$$

$$\left[TE_1(\rho_0^*, \mathbf{q}^*, P^*) - T\rho_1^* Q_1^*, \dots, TE_K(\rho_0^*, \mathbf{q}^*, P^*) - T\rho_K^* Q_K^* \right],$$

where $R^* = 0$ is chosen for simplicity.

3) *Constructing Optimal Primal Solution to (P2.1):* With λ^{opt} and μ^{opt} at hand, it remains to construct the optimal primal solution to (P2.1), denoted by $\{\rho_k^{\text{opt}}(t), P^{\text{opt}}(t), Q_k^{\text{opt}}(t), \mathbf{q}^{\text{opt}}(t)\}$ and R^{opt} . Before proceeding, we have the following proposition.

Proposition 3.2: At the optimal λ^{opt} and μ^{opt} , it must hold that $\phi(\{\bar{\mathbf{q}}_{\omega}^{(\mu^{\text{opt}})}\}, P_{\text{peak}}, \{\mu_k^{\text{opt}}\}) = \varphi_k(\mathbf{w}_k, Q^{(\lambda_k^{\text{opt}}, \mu_k^{\text{opt}})}, \lambda_k^{\text{opt}}, \mu_k^{\text{opt}}), \forall k \in \mathcal{K}, \forall \omega \in \{1, \dots, \Omega^{(\mu^{\text{opt}})}\}$.

By combining Propositions 3.1 and 3.2, it is suggested that under optimal dual solution λ^{opt} and μ^{opt} to (D2.1), problem (18) has a total number of $\Omega^{(\mu^{\text{opt}})} + K$ non-unique optimal solutions. Among them, the $\Omega^{(\mu^{\text{opt}})}$ optimal solutions are given in (21), and the other K solutions are given in (22) (each for one user k). In this case, we need to time-share among these non-unique optimal solutions to construct the optimal primal solution to (P2.1).

More specifically, notice that the $\Omega^{(\mu^{\text{opt}})}$ solutions in (21) correspond to $\Omega^{(\mu^{\text{opt}})}$ hovering locations $\bar{\mathbf{q}}_1^{(\mu^{\text{opt}})}, \dots, \bar{\mathbf{q}}_{\Omega^{(\mu^{\text{opt}})}}^{(\mu^{\text{opt}})}$ for downlink WPT, at which only the UAV transmits with $P^* = P_{\text{peak}}$ and $\rho_0^* = 1$; on the other hand, the k -th solutions in (22), $k \in \mathcal{K}$, corresponds to that the UAV hovers above user k at location \mathbf{w}_k for uplink WIT, at which user k transmits with $Q_k^* = Q^{(\lambda_k^{\text{opt}}, \mu_k^{\text{opt}})}$ and $\rho_k^* = 1$. With time-

sharing, let τ_ω and ς_k denote the hovering duration at the location $\bar{\mathbf{q}}_\omega^{(\mu^{\text{opt}})}$, $\omega \in \{1, \dots, \Omega^{(\mu^{\text{opt}})}\}$ and $\mathbf{w}_k, k \in \{1, \dots, K\}$, respectively. In this case, we can solve the following uplink common throughput maximization problem to obtain the optimal hovering durations τ_ω 's and ς_k 's for time sharing.

$$\begin{aligned}
 \text{(P2.2)}: \quad & \max_{\{\varsigma_k \geq 0, \tau_\omega \geq 0\}, R} R \\
 \text{s.t.} \quad & \varsigma_k \log_2 \left(1 + \frac{Q^{(\lambda_k^{\text{opt}}, \mu_k^{\text{opt}})} \gamma}{H^2} \right) \geq R, \forall k \in \mathcal{K} \\
 & \varsigma_k Q^{(\lambda_k^{\text{opt}}, \mu_k^{\text{opt}})} \leq \sum_{\omega=1}^{\Omega^{(\mu^{\text{opt}})}} \frac{\tau_\omega \eta P_{\text{peak}} \beta_0}{\|\bar{\mathbf{q}}_\omega^{(\mu^{\text{opt}})} - \mathbf{w}_k\|^2 + H^2}, \forall k \in \mathcal{K} \\
 & \sum_{k=1}^K \varsigma_k + \sum_{\omega=1}^{\Omega} \tau_\omega = T.
 \end{aligned}$$

Note that problem (P2.2) is a linear program, which can be solved by standard convex optimization techniques in [18]. The optimal solution to (P2.2) is denoted as $\{\hat{\varsigma}_k, \hat{\tau}_\omega\}$ and \hat{R} . Accordingly, we can divide the whole period \mathcal{T} into $\Omega^{(\mu^{\text{opt}})} + K$ sub-periods, where the first $\Omega^{(\mu^{\text{opt}})}$ sub-periods, denoted by $\mathcal{T}_\omega = (\sum_{j=1}^{\omega-1} \hat{\tau}_j, \sum_{j=1}^\omega \hat{\tau}_j]$, $\forall \omega \in \{1, \dots, \Omega^{(\mu^{\text{opt}})}\}$, are for downlink WPT, and the next K sub-periods, denoted by $\mathcal{T}_{\Omega^{(\mu^{\text{opt}})}+k} = (\sum_{\omega=1}^{\Omega^{(\mu^{\text{opt}})}} \hat{\tau}_\omega + \sum_{j=1}^{k-1} \hat{\varsigma}_j, \sum_{\omega=1}^{\Omega^{(\mu^{\text{opt}})}} \hat{\tau}_\omega + \sum_{j=1}^k \hat{\varsigma}_j]$, $\forall k \in \mathcal{K}$, are for uplink WIT of the K users. As a result, we have the following proposition.

Proposition 3.3: The optimal solution to (P2.1) (and thus (P2)) is given as follows. During sub-period $\omega \in \{1, \dots, \Omega^{(\mu^{\text{opt}})}\}$, the UAV hovers at the location $\bar{\mathbf{q}}_\omega^{(\mu^{\text{opt}})}$ for downlink WPT, i.e.,

$$\begin{aligned}
 \mathbf{q}^{\text{opt}}(t) &= \bar{\mathbf{q}}_\omega^{(\mu^{\text{opt}})}, \rho_0^{\text{opt}}(t) = 1, \rho_k^{\text{opt}}(t) = 0, \\
 P^{\text{opt}}(t) &= P_{\text{peak}}, Q_k^{\text{opt}}(t) = 0, \forall k \in \mathcal{K},
 \end{aligned} \tag{23}$$

$\forall t \in \mathcal{T}_\omega, \omega \in \{1, \dots, \Omega^{(\mu^{\text{opt}})}\}$. During sub-period $\Omega^{(\mu^{\text{opt}})} + k$, $k \in \{1, \dots, K\}$, the UAV hovers above user k at \mathbf{w}_k , and user k sends information to the UAV in the uplink, i.e.,

$$\begin{aligned}
 \mathbf{q}^{\text{opt}}(t) &= \mathbf{w}_k, \rho_k^{\text{opt}}(t) = 1, Q_k^{\text{opt}}(t) = Q^{(\lambda_k^{\text{opt}}, \mu_k^{\text{opt}})}, P^{\text{opt}}(t) = 0, \\
 \rho_j^{\text{opt}}(t) &= 0, Q_j^{\text{opt}}(t) = 0, \forall j \in \{0\} \cup \mathcal{K}, j \neq k,
 \end{aligned} \tag{24}$$

$\forall t \in \mathcal{T}_{\Omega^{(\mu^{\text{opt}})}+k}, k \in \{1, \dots, K\}$. The optimal uplink common throughput is given as $R^{\text{opt}} = \hat{R}$ (with $R^{\text{opt}} = \hat{R}$ is the optimal solution obtained for (P2.2)).

IV. PROPOSED SOLUTION TO PROBLEM (P1)

This section considers problem (P1) with the maximum UAV speed constraint in (2). We first present a successive hover-and-fly trajectory based on the multi-location-hovering solution to the relaxed problem (P2), and then design the wireless resource allocation for (P1) by discretizing the time period.

A. Successive Hover-and-Fly Trajectory Design

First, we propose the successive hover-and-fly trajectory design, in which the UAV sequentially visits the $\Omega^{(\mu^{\text{opt}})} + K$ optimal hovering locations that are obtained for (P2), i.e., $\bar{\mathbf{q}}_1^{(\mu^{\text{opt}})}, \dots, \bar{\mathbf{q}}_{\Omega^{(\mu^{\text{opt}})}}^{(\mu^{\text{opt}})}$ for downlink WPT, and $\mathbf{w}_1, \dots, \mathbf{w}_K$ for uplink WIT. For notational convenience, we denote the

$\Omega^{(\mu^{\text{opt}})} + K$ hovering locations as $\{\mathbf{q}_k^{\text{opt}}\}$, where $\mathbf{q}_k^{\text{opt}} = \bar{\mathbf{q}}_k^{(\mu^{\text{opt}})}$, $\forall k \in \{1, \dots, \Omega^{(\mu^{\text{opt}})}\}$, and $\mathbf{q}_{\Omega^{(\mu^{\text{opt}})}+k}^{\text{opt}} = \mathbf{w}_k, \forall k \in \{1, \dots, K\}$. In order to maximize the time for efficient WPT and WIT, the UAV flies among these hovering locations by using the maximum speed V_{max} , and the UAV aims to minimize the flying time by equivalently minimizing the travelling path among the $\Omega^{(\mu^{\text{opt}})} + K$ locations.

First, we obtain the travelling path to minimize the flying distance to visit all the $\Omega^{(\mu^{\text{opt}})} + K$ hovering locations. We define a set of binary variables $f_{j,k}$, $\forall j, k \in \{1, \dots, \Omega^{(\mu^{\text{opt}})} + K\}, j \neq k$, where $f_{j,k} = 1$ or $f_{j,k} = 0$ indicates that the UAV flies or does not fly from the j -th hovering location $\mathbf{q}_j^{\text{opt}}$ to the k -th hovering location $\mathbf{q}_k^{\text{opt}}$. Hence, the travelling path minimization problem becomes determining $\{f_{j,k}\}$ to minimize $\sum_{j=1}^{\Omega^{(\mu^{\text{opt}})}+K} \sum_{k=1, k \neq j}^{\Omega^{(\mu^{\text{opt}})}+K} f_{j,k} d_{j,k}$, provided that each of the $\Omega^{(\mu^{\text{opt}})} + K$ locations is visited once, where $d_{j,k} = \|\mathbf{q}_j^{\text{opt}} - \mathbf{q}_k^{\text{opt}}\|$ denotes the distance between $\mathbf{q}_j^{\text{opt}}$ and $\mathbf{q}_k^{\text{opt}}$. Note that as shown in [15], the flying distance minimization can be equivalently solved by a well-established travelling salesman problem (TSP), for which the details are omitted here for brevity. In this case, we use the permutation $\kappa(\cdot)$ over the set $\{1, \dots, \Omega^{(\mu^{\text{opt}})} + K\}$ to denote the obtained travelling path, where the $\kappa(1)$ -th hovering location is first visited, followed by the $\kappa(2)$ -th, the $\kappa(3)$ -th, etc., until the last $\kappa(K + \Omega^{(\mu^{\text{opt}})})$ -th one. We denote the distance and travelling duration from the $\kappa(i)$ -th hovering location $\mathbf{q}_{\kappa(i)}^{\text{opt}}$ to the $\kappa(i+1)$ -th hovering location $\mathbf{q}_{\kappa(i+1)}^{\text{opt}}$ as $d_{\kappa(i), \kappa(i+1)}$ and $T_{\text{fly},i} = d_{\kappa(i), \kappa(i+1)} / V_{\text{max}}$, respectively, $\forall i \in \{1, \dots, \Omega^{(\mu^{\text{opt}})} + K - 1\}$. Hence, the total travelling distance and duration are given as $D_{\text{fly}} = \sum_{i=1}^{\Omega^{(\mu^{\text{opt}})}+K-1} d_{\kappa(i), \kappa(i+1)}$, and $T_{\text{fly}} = D_{\text{fly}} / V_{\text{max}}$, respectively. We denote the obtained flying trajectory as $\{\tilde{\mathbf{q}}(t)\}_{t=0}^{T_{\text{fly}}}$.

To obtain the complete hover-and-fly trajectory, we still need to determine the hovering durations at the $\Omega^{(\mu^{\text{opt}})} + K$ hovering locations.² Let τ_ω denote the time duration for the UAV to hover at the location $\mathbf{q}_\omega^{\text{opt}} = \bar{\mathbf{q}}_\omega^{(\mu^{\text{opt}})}$ for WPT, $\omega \in \{1, \dots, \Omega^{(\mu^{\text{opt}})}\}$, and ς_k denote the the time duration for the UAV to hover above user k at $\mathbf{q}_{\Omega^{(\mu^{\text{opt}})}+k}^{\text{opt}} = \mathbf{w}_k$ for WIT, $k \in \{1, \dots, K\}$. Furthermore, we define

$$\zeta_k \triangleq \begin{cases} \tau_{\kappa(k)}, & \text{if } \kappa(k) \in \{1, \dots, \Omega^{(\mu^{\text{opt}})}\} \\ \varsigma_{\kappa(k)-\Omega^{(\mu^{\text{opt}})}}, & \text{if } \kappa(k) \in \{\Omega^{(\mu^{\text{opt}})} + 1, \dots, \Omega^{(\mu^{\text{opt}})} + K\}. \end{cases}$$

Accordingly, we can divide the time duration into $2(\Omega^{(\mu^{\text{opt}})} + K) - 1$ sub-phases, denoted by $[\hat{\mathcal{T}}_1, \hat{\mathcal{T}}_2, \dots, \hat{\mathcal{T}}_{2(\Omega^{(\mu^{\text{opt}})}+K)-1}]$, which are defined as

$$\hat{\mathcal{T}}_{2k-1} \triangleq \left(\sum_{i=1}^{k-1} (\zeta_{\kappa(i)} + T_{\text{fly},i}), \sum_{i=1}^{k-1} (\zeta_{\kappa(i)} + T_{\text{fly},i}) + \zeta_{\kappa(k)} \right]$$

for odd sub-periods with $k \in \{1, \dots, \Omega^{(\mu^{\text{opt}})} + K\}$, and

$$\hat{\mathcal{T}}_{2k} \triangleq \left(\sum_{i=1}^{k-1} (\zeta_{\kappa(i)} + T_{\text{fly},i}) + \zeta_{\kappa(k)}, \sum_{i=1}^k (\zeta_{\kappa(i)} + T_{\text{fly},i}) \right]$$

for even sub-periods with $k \in \{1, \dots, \Omega^{(\mu^{\text{opt}})} + K - 1\}$. Therefore, within each odd sub-period $2k-1$, the UAV should

²In order for the UAV to visit all the $\Omega^{(\mu^{\text{opt}})} + K$ hovering locations, we consider $T \geq T_{\text{fly}}$ in this paper, and leave the case with $T < T_{\text{fly}}$ in the journal version of this paper.

hover at the $\kappa(k)$ -th hovering location $(x_{\kappa(k)}, y_{\kappa(k)}, H)$, i.e.,

$$\mathbf{q}(t) = \mathbf{q}_{\kappa(k)}^{\text{opt}}, \quad (25)$$

$\forall t \in \hat{\mathcal{T}}_{2k-1}, k \in \{1, \dots, \Omega^{(\mu^{\text{opt}})} + K\}$. During each even sub-period $2k$, the UAV should fly from the $\kappa(k)$ -th hovering location to $\kappa(k+1)$ -th hovering location with maximum UAV speed V_{\max} , whose time-varying location is

$$\mathbf{q}(t) = \tilde{\mathbf{q}} \left(t - \sum_{i=1}^k \zeta_{\kappa(i)} \right), \quad (26)$$

$\forall t \in \hat{\mathcal{T}}_{2k}, k \in \{1, \dots, \Omega^{(\mu^{\text{opt}})} + K - 1\}$. Therefor, the successive hover-and-fly trajectory is obtained, in which the hovering durations $\{\zeta_{\kappa(k)}\}$, or equivalently, $\{\tau_{\omega}\}$ and $\{\varsigma_k\}$, are optimization variables that will be determined next.

B. Wireless Resource Allocation Under Successive Hover-and-Fly Trajectory

Under the obtained successive hover-and-fly trajectory, we maximize the uplink common throughput of all users by optimizing the transmission mode $\{\rho_k(t)\}$ and the power allocation $\{P(t)\}$ and $\{Q_k(t)\}$, jointly with the hovering durations $\{\tau_{\omega}\}$ and $\{\varsigma_k\}$. Towards this end, we first discuss the transmission policy of the UAV-enabled WPCN during each sub-period.

First, consider the $(2k-1)$ -th sub-phase $\hat{\mathcal{T}}_{2k-1}, \forall k \in \{1, \dots, \Omega^{(\mu^{\text{opt}})} + K\}$, in which the UAV hovers above $\mathbf{q}_{\kappa(k)}^{\text{opt}}$ as in (25). The transmission policy in this sub-phase is based on the optimal solution to (P2) in Section III. In particular, if $1 \leq \kappa(k) \leq \Omega^{(\mu^{\text{opt}})}$, we denote $\omega = \kappa(k)$ for convenience. In this case, the UAV hovers at $\bar{\mathbf{q}}_{\omega}^{(\mu^{\text{opt}})}$ with duration τ_{ω} , and the UAV works in the downlink WPT during this sub-phase, by employing an unchanged transmit power, denoted by $P_{\omega}^{\text{hover}}$. On the other hand, if $\Omega^{(\mu^{\text{opt}})} + 1 \leq \kappa(k) \leq \Omega^{(\mu^{\text{opt}})} + K$, we denote $\hat{k} = \kappa(k) - \Omega^{(\mu^{\text{opt}})}$. In this case, the UAV hovers above user \hat{k} at $\mathbf{w}_{\hat{k}}$ with duration $\varsigma_{\hat{k}}$, and user \hat{k} works in the uplink WIT to the UAV during the whole sub-phase, by employing an unchanged transmit power, denoted by $Q_{\hat{k}}^{\text{hover}}$. By combining the $(\Omega^{(\mu^{\text{opt}})} + K)$ odd sub-phases, the uplink throughput and the harvested energy at each user k are respectively given as

$$\widetilde{R}_k(\varsigma_k, Q_k^{\text{hover}}) = \varsigma_k \log_2 \left(1 + \frac{h_k(\mathbf{w}_k) Q_k^{\text{hover}}}{\sigma^2} \right) \quad (27)$$

$$\widetilde{E}_k(\{\tau_{\omega}, P_{\omega}^{\text{hover}}\}) = \sum_{\omega=1}^{\Omega^{(\mu^{\text{opt}})}} \eta h_k(\bar{\mathbf{q}}_{\omega}^{(\mu^{\text{opt}})}) \tau_{\omega} P_{\omega}^{\text{hover}}. \quad (28)$$

Next, consider the even sub-phases $\hat{\mathcal{T}}_{2k}, \forall k \in \{1, \dots, \Omega^{(\mu^{\text{opt}})} + K - 1\}$, with a total duration of T_{fly} . We discretize these sub-phases into N slots each with duration $\delta = T_{\text{fly}}/N$. For each slot $n \in \mathcal{N} \triangleq \{1, \dots, N\}$, the location of the UAV is constant and denoted as $\mathbf{q}^{\text{fly}}[n] = \tilde{\mathbf{q}}(n\delta)$. Furthermore, in order to handle the binary transmission mode indicator $\{\rho_k(t)\}$, we consider that the $(K+1)$ transmission modes are time shared within one slot, by dividing each slot n into $(K+1)$ sub-slots. In the first sub-slot with duration $\tau_0^{\text{fly}}[n] \geq 0$, the UAV works in the downlink WPT mode by using a transmit power $P^{\text{fly}}[n]$, and in sub-slot $k+1$ with duration $\tau_k^{\text{fly}}[n] \geq 0$, user k works in the uplink WIT by

using transmit power $Q_k^{\text{fly}}[n], \forall k \in \mathcal{K}$. Here, it follows that $\sum_{k=0}^K \tau_k^{\text{fly}}[n] = \delta, \forall n \in \mathcal{N}$. By combining the N slots of the even sub-periods, the uplink throughput and the harvested energy at each user k are respectively given as

$$R_k^{\text{fly}}(\{\tau_k^{\text{fly}}[n], Q_k^{\text{fly}}[n]\}) = \sum_{n \in \mathcal{N}} \tau_k^{\text{fly}}[n] \log_2 \left(1 + \frac{h_k(\mathbf{q}^{\text{fly}}[n]) Q_k^{\text{fly}}[n]}{\sigma^2} \right), \quad (29)$$

$$E_k^{\text{fly}}(\{\tau_0^{\text{fly}}[n], P^{\text{fly}}[n]\}) = \sum_{n \in \mathcal{N}} \eta h_k(\mathbf{q}^{\text{fly}}[n]) \tau_0^{\text{fly}}[n] P^{\text{fly}}[n]. \quad (30)$$

Based on (27), (28), (29), and (30), the uplink common throughput maximization problem is reformulated as the following problem (P3), in which the optimization variables include $\{\varsigma_k\}$, $\{Q_k^{\text{hover}}\}$, $\{\tau_{\omega}\}$, $\{P_{\omega}^{\text{hover}}\}$, $\{\tau_k^{\text{fly}}[n]\}$, $\{Q_k^{\text{fly}}[n]\}$, $\{P^{\text{fly}}[n]\}$, and R .

$$(P3): \max R$$

$$\begin{aligned} \text{s.t. } & \widetilde{R}_k(\varsigma_k, Q_k^{\text{hover}}) + R_k^{\text{fly}}(\{\tau_k^{\text{fly}}[n], Q_k^{\text{fly}}[n]\}) \geq R, \forall k \in \mathcal{K} \\ & \varsigma_k Q_k^{\text{hover}} + \sum_{n=1}^N \tau_k[n] Q_k^{\text{fly}}[n] \leq \widetilde{E}_k(\{\tau_{\omega}, P_{\omega}^{\text{hover}}\}) \\ & \quad + E_k^{\text{fly}}(\{\tau_0^{\text{fly}}[n], P^{\text{fly}}[n]\}), \forall k \in \mathcal{K} \\ & \varsigma_k \geq 0, \forall k \in \mathcal{K}, \tau_{\omega} \geq 0, \forall \omega \in \{1, \dots, \Omega^{(\mu^{\text{opt}})}\} \end{aligned} \quad (31)$$

$$\sum_{k=1}^K \varsigma_k + \sum_{\omega=1}^{\Omega^{(\mu^{\text{opt}})}} \tau_{\omega} = T - T^{\text{fly}} \quad (32)$$

$$\tau_k^{\text{fly}}[n] \geq 0, \forall n \in \mathcal{N}, k \in \mathcal{K} \cup \{0\} \quad (33)$$

$$\sum_{k=0}^K \tau_k^{\text{fly}}[n] = \delta, \forall n \in \mathcal{N}. \quad (34)$$

Note that although problem (P3) is non-convex due to the coupling between some variables (e.g., between ς_k and Q_k^{hover}). Fortunately, via change of variables (e.g., introducing $E_k^{\text{hover}} = \varsigma_k Q_k^{\text{hover}}$), we can transform problem (P3) into a convex optimization problem, which can thus be solved via standard convex optimization techniques. By combining the optimal solution to (P3) together with the successive hover-and-fly trajectory in (25) and (26), the solution to (P1) is finally found.

Remark 4.1: It is worth noting that the proposed successive hover-and-fly trajectory design is asymptotically optimal for problem (P1), as the flying time becomes negligible as compared to the hovering time. In this case, the obtained uplink common throughput approaches the optimal value of (P2), which serves as the upper bound of that of (P1).

V. NUMERICAL RESULTS

In this section, we present numerical results to validate the performance of our proposed trajectory designs as compared to the following banchmark scheme, with static UAV hovering. In this benchmark scheme, the UAV statically hovers at an optimized location $(x^{\text{static}}, y^{\text{static}}, H)$ to maximize the uplink common throughput of all users. $(x^{\text{static}}, y^{\text{static}})$ can be obtained by solving the problem (P2) under given fixed UAV location, together with a 2D exhaustive search.

In the simulation, we consider a system with $K = 9$ ground users that are randomly distributed within a 2D area of $20 \times 20 \text{ m}^2$, as shown in Fig. 2. And the UAV flies at a fixed altitude

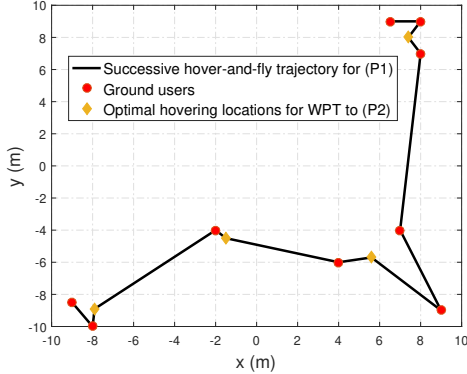


Fig. 2. System setup for simulation.

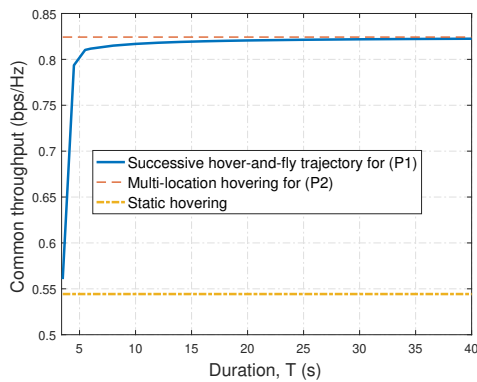


Fig. 3. Uplink common throughput versus the time duration T .

$H = 5$ m. The receiver noise power is assumed to be $\sigma^2 = -70$ dBm. The channel power gain at the reference distance $d_0 = 1$ m is set as $\beta_0 = -30$ dB. The energy harvesting efficiency is set as $\eta = 50\%$. The maximum speed of the UAV is $V_{\max} = 10$ m/s.

For illustration, Fig. 2 shows the optimal hovering locations for problem (P2), and the successive hover-and-fly trajectory under the 9-user setup, in which $T = 40$ s and $P_{\text{peak}} = 100$ W. It is observed that there are $\Omega^{(\mu^{\text{opt}})} = 4$ optimal hovering locations for WPT and a total of $\Omega^{(\mu^{\text{opt}})} + K = 13$ optimal hovering locations to problem (P2).

Fig. 3 shows the uplink common throughput of the K users versus the time duration T , in which $P_{\text{peak}} = 100$ W. It is observed that the proposed successive hover-and-fly trajectory (jointly with the optimal wireless resource allocation) achieves higher common throughput than the static-hoovering benchmark, and the performance gain becomes more substantial when T becomes larger. Furthermore, with a large T value, the successive hover-and-fly trajectory is observed to have a similar performance as the upper bound by the multi-location-hoovering solution to (P2) with the maximum UAV speed constraint ignored. This is consistent with Remark 4.1.

VI. CONCLUSION

In this paper, we investigated the common throughput maximization problem in a new UAV-enabled WPCN, subject

to the UAV's maximum speed constraint and the users' energy harvesting constraints. We jointly optimized the UAV trajectory and the wireless resource allocation in both downlink WPT and uplink WIT. To solve this difficult problem, we first considered the special case with the maximum UAV speed constraint dropped and solved the relaxed problem globally optimally. The optimal solution showed that the UAV should hover over two sets of optimal hovering locations for downlink WPT and uplink WIT, respectively. Next, based on the optimal solution to the above relaxed problem, we proposed a successive hover-and-fly trajectory design to solve the general problem with the maximum UAV speed constraint considered. Numerical results showed that the proposed design achieves near-optimal performance.

REFERENCES

- [1] S. Bi, C. K. Ho, and R. Zhang, "Wireless powered communication: Opportunities and challenges," *IEEE Commun. Mag.*, vol. 53, no. 4, pp. 117–125, Apr. 2015.
- [2] H. Ju and R. Zhang, "Throughput maximization in wireless powered communication networks," *IEEE Trans. Wireless Commun.*, vol. 13, no. 1, pp. 418–428, Jan. 2014.
- [3] J. Xu and R. Zhang, "Energy beamforming with one-bit feedback," *IEEE Trans. Signal Process.*, vol. 62, no. 20, pp. 5370–5381, Oct. 2014.
- [4] J. Xu, L. Liu, and R. Zhang, "Multiuser MISO beamforming for simultaneous wireless information and power transfer," *IEEE Trans. Signal Process.*, vol. 62, no. 18, pp. 4798–4810, Sep. 2014.
- [5] J. Xu and R. Zhang, "A general design framework for MIMO wireless energy transfer with limited feedback," *IEEE Trans. Signal Process.*, vol. 64, no. 10, pp. 2475–2488, May 2016.
- [6] Y. Che, J. Xu, L. Duan, and R. Zhang, "Multiantenna wireless powered communication with co-channel energy and information transfer," *IEEE Commun. Lett.*, vol. 19, no. 12, pp. 2266–2269, Dec. 2015.
- [7] H. Ju and R. Zhang, "User cooperation in wireless powered communication networks," in *Proc. IEEE Globecom*, 2014.
- [8] H. Chen, Y. Li, J. L. Rebelatto, B. F. U. Filho, and B. Vucetic, "Harvest-then-cooperate: Wireless-powered cooperative communications," *IEEE Trans. Signal Process.*, vol. 63, no. 7, pp. 1700–1711, Apr. 2015.
- [9] Y. Zeng, R. Zhang, and T. J. Lim, "Wireless communications with unmanned aerial vehicles: Opportunities and challenges," *IEEE Commun. Mag.*, vol. 54, no. 5, pp. 36–42, May 2016.
- [10] Y. Zeng, R. Zhang, and T. J. Lim, "Throughput maximization for UAV-enabled mobile relaying systems," *IEEE Trans. Commun.*, vol. 64, no. 12, pp. 4983–4996, Dec. 2016.
- [11] J. Lyu, Y. Zeng, R. Zhang, and T. J. Lim, "Placement optimization of UAV-mounted mobile base stations," *IEEE Commun. Lett.*, vol. 21, no. 3, pp. 604–607, Mar. 2017.
- [12] R. I. Bor-Yaliniz, A. El-Keyi, and H. Yanikomeroglu, "Efficient 3-D placement of an aerial base station in next generation cellular networks," in *Proc. IEEE ICC*, pp. 1–5, 2016.
- [13] M. Mozaffari, W. Saad, M. Bennis, and M. Debbah, "Efficient deployment of multiple unmanned aerial vehicles for optimal wireless coverage," *IEEE Commun. Lett.*, vol. 20, no. 8, pp. 1647–1650, 2016.
- [14] Q. Wu, Y. Zeng, and R. Zhang, "Joint trajectory and communication design for UAV-enabled multiple access," [Online] Available: <https://arxiv.org/abs/1704.01765>
- [15] J. Xu, Y. Zeng, and R. Zhang, "UAV-enabled wireless power transfer: Trajectory design and energy optimization," submitted to *IEEE Trans. Wireless Commun.*, [Online] Available: <https://arxiv.org/abs/1706.07010>
- [16] J. Xu, Y. Zeng, and R. Zhang, "UAV-enabled wireless power transfer: Trajectory design and energy region characterization," *IEEE Global Communications Conference (Globecom) Workshop*, 2017.
- [17] W. Yu and R. Lui, "Dual methods for nonconvex spectrum optimization of multicarrier systems," *IEEE Trans. Commun.*, vol. 54, no. 7, pp. 1310–1322, 2006.
- [18] S. Boyd and L. Vandenberghe, *Convex Optimization*, Cambridge, U.K.: Cambridge Univ. Press, Mar. 2004.